24th INTERNATIONAL CONGRESS ON SOUND AND VIBRATION
23–27 July 2017, London

ICSV24
23-27JULY 2017
LONDON CALLING

SIMPLIFIED ONE-DIMENSIONAL MODEL FOR TRANSIENT TIME-DOMAIN SIMULATION OF CENTRIFUGAL PUMPS

Andreas Linkamp, Christian Lehr and Andreas Brümmer
Chair of Fluidics, TU Dortmund University, Dortmund, Germany
email: andreas.linkamp@tu-dortmund.de

In the present work a one-dimensional time-domain model of centrifugal pumps is presented. The acoustic excitation and transmission characteristics as well as the steady behaviour of cavitation-free pumps are comprised in this model. Assuming solely plane wave propagation, the pump's acoustic transmission properties are modelled by a reduced one-dimensional representation of the complex impeller and volute geometry. The acoustic excitation consists of the superposition of a monopole and a dipole source in the tongue region at the outlet of the pump. The amplitudes and the phasing of these sources are obtained empirically by means of pressure measurements on the suction and discharge side of the modelled pump. Regarding the steady behaviour, the characteristic curve is included in the model such that, in combination with the piping model of a plant, the respective mean flow conditions are realised in a simulation. Such a model allows integral simulation of the acoustic excitation and transmission characteristics of centrifugal pumps and the system response. Due to the time-domain formulation time-variant behaviour such as opening or closing of valves can be considered. A first validation of the pump model is carried out in an exemplary operating point under cavitation-free conditions.

Keywords: centrifugal pumps, hydroacoustics, hydraulic systems

1. Introduction

In centrifugal pumps pressure and velocity pulsations are excited due to non-uniform pressure and velocity distribution along the impeller outlet, which interact which the volute tongue [1, 2]. These pulsations can lead to vibration in the piping system and increased noise emission. The quantity of the excitation is strongly influenced by the geometry in the vicinity of the tongue [3, 4] as well as operating parameters such as rotational speed and operating point [2, 5, 6]. Occuring pressure amplitudes in connected piping systems result from the pump's pulsation excitation and acoustic transmission properties as well as the piping system's response to the pulsations induced by the pump [7, 8]. Therefore it is of high interest to model the transient behaviour of centrifugal pumps in order to predict the pulsations in arbitrary connected piping systems.

Basically two different approaches to model the transient behaviour of centrifugal pumps are carried out in literature: one approach is formulated in the frequency domain and consist of a four-pole matrix modelling the transmission behaviour and a source vector for the excitation of a pump. The four-pole parameters of such a model are either obtained by means of geometrical and material parameters of the pump based on electro-acoustic analogy [9, 10] or by direct measurement of the components of transfer or scattering matrices [7, 11]. The source vector is usually determined by means of experimental investigations. The major advantage of such models is the simple formulation. The interaction of a pump with piping systems can usually be obtained analytically, thus in the vicinity of a known pump occuring pulsations can be calculated directly. However there are several drawbacks

of models in the frequency-domain which are necessarily linear time-invariant (LTI) systems. Due to the linear formulation, non-linear effects such as cavitation or amplitude-dependent damping of a bladder accumulator can not be taken into account. Furthermore, since models in the frequency domain are usually time-invariant, time-dependent problems like e.g. a closing valve can not be modelled.

The other approach is based on numerical time-domain simulations instead of experiments. These are usually carried out in three dimensions. A series of investigations has been carried out to numerically investigate the pulsation excitation of centrifugal pumps, e.g. [4, 12]. By means of a two-way-coupling the mutual interaction between the hydrodynamic field in the pump and the hydroacoustic field in connected piping systems can be taken into account [13]. However, CFD calculations of complex flows such as the flow in a centrifugal pump is rather suitable for parametric studies or to gain understanding of occuring effects than for reliable quantitative predictions of occuring pressure pulsations [4]. Furthermore, full threedimensional unsteady simulations require high computational resources and time.

In the present work a reduced onedimensional numerical model for a centrifugal pump formulated in the time-domain is presented. The model contains the acoustic excitation and transmission characteristics as well as the stationary energy conversion given by the characteristic head curve. Due to the time-domain formulation nonlinear effects and time-variant components can be taken into account. Furthermore, the reduction to one spatial dimension leads to fast computations of complete piping systems. The acoustical parameters are obtained experimentally.

2. One-dimensional model

The presented model is based on the non-linear onedimensional conservation equations for mass and momentum in characteristic form [14]:

$$\frac{dp}{dt} + \rho a \frac{dc}{dt} = 0 \quad \text{along} \quad \frac{dx}{dt} = c + a \tag{1}$$

$$\frac{dp}{dt} - \rho a \frac{dc}{dt} = 0 \quad \text{along} \quad \frac{dx}{dt} = c - a \tag{2}$$

Isothermal and inviscid flow is assumed.The numerical solution is carried out using a finite-difference scheme with first order upwind discretisation. For temporal discretisation, an explicit Euler scheme is applied. The flow variables pressure p and velocity c at grid point i and time step $n+1$ are obtained by:

$$p_i^{(n+1)} = \frac{1}{2}\left(\rho_i^n a_i^n \left(c_A - c_B\right) + \left(p_A + p_B\right)\right) \tag{3}$$

$$c_i^{(n+1)} = \frac{1}{2}\left(\frac{1}{\rho_i^n a_i^n}\left(p_A - p_B\right) + \left(c_A + c_B\right)\right) \tag{4}$$

The subscripts A/B denote the values at the base points for the two sound characteristics (A/B) at timestep n, whereby base point A is between grid point $i-1$ and i and base point B is located between grid point i and $i+1$, cf Fig. 1.

2.1 Pump

In order to represent a centrifugal pump's acoustic behaviour, two properties have to be modelled, namely the acoustic transmission behaviour and the acoustic excitation on the downstream (discharge) side. These parameters are obtained experimentally, evaluated in the frequency domain and then transformed into the time domain for the model presented in this work. A well-known representation

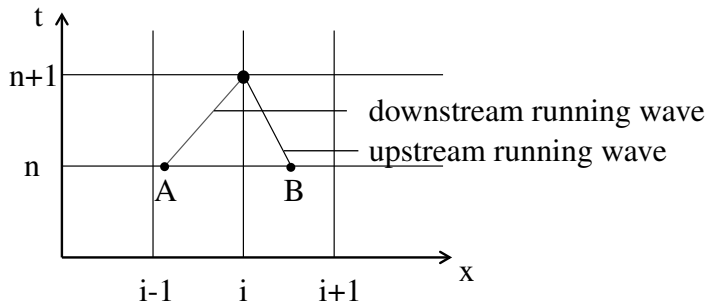

Figure 1: Time-space-grid with indicated base points A/B for positive direction of flow.

for a pump in the frequency domain is expressed by means of the transmission matrix $\bar{\bar{T}}$:

$$\begin{pmatrix} \hat{\underline{f}}_d \\ \hat{\underline{g}}_d \end{pmatrix} = \bar{\bar{T}} \cdot \begin{pmatrix} \hat{\underline{f}}_u \\ \hat{\underline{g}}_u \end{pmatrix} + \begin{pmatrix} \hat{\underline{f}}_s \\ \hat{\underline{g}}_s \end{pmatrix} \tag{5}$$

The Riemann invariants $\hat{\underline{f}}$ and $\hat{\underline{g}}$ represent the complex amplitudes of acoustic waves running in downstream and upstream direction. The acoustic field of primitive variables is related to the Riemann invariants by [15]:

$$\hat{\underline{f}} = \frac{1}{2}\left(\frac{\hat{\underline{p}}}{\rho a} + \hat{\underline{c}}\right) \tag{6}$$

$$\hat{\underline{g}} = \frac{1}{2}\left(\frac{\hat{\underline{p}}}{\rho a} - \hat{\underline{c}}\right) \tag{7}$$

The transmission matrix $\bar{\bar{T}}$ connects the Riemann invariants on the the upstream (u) and the downstream side (d) of the pump. Furthermore, a source vector (subscript s) is comprised which represents the acoustic excitation. A schematic onedimensional time domain model representing the system in Eq.(5) is illustrated in Fig.2.

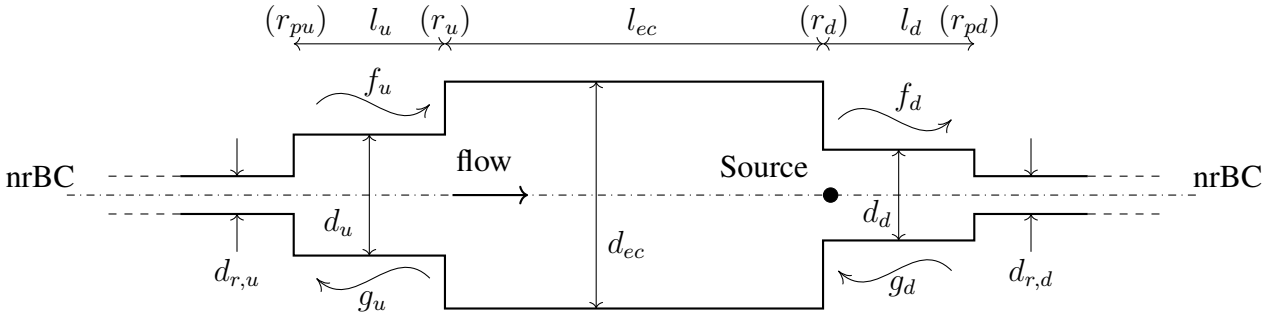

Figure 2: Schematic of the pump and piping impedance model.

The transmission behaviour is approximated by a simple expansion chamber located between the upstream (suction) and downstream (discharge) piping. Each section is assumed as a pipe with constant cross section and calculated by the scheme described above. The flow variables at the cross sectional jumps are obtained by extending the system of characteristic equations Eqs.(1–2) with a mass conservation and a total pressure balance. The transmission properties of a four-pole can also be expressed in terms of the scattering matrix $\bar{\bar{S}}$, which is the form used in the present work [10].

$$\begin{pmatrix} \hat{\underline{f}}_d \\ \hat{\underline{g}}_u \end{pmatrix} = \bar{\bar{S}} \begin{pmatrix} \hat{\underline{f}}_u \\ \hat{\underline{g}}_d \end{pmatrix} = \begin{pmatrix} \underline{t}_{ud} & \underline{r}_d \\ \underline{r}_u & \underline{t}_{du} \end{pmatrix} \begin{pmatrix} \hat{\underline{f}}_u \\ \hat{\underline{g}}_d \end{pmatrix} \tag{8}$$

The two free geometrical parameters of the expansion chamber l_{ec} and d_{ec} define the complex transmission properties. These parameters are chosen in such a way, that the transmission properties of the expansion chamber correspond to those experimentally obtained for the centrifugal pump as will be shown in Section 3.
The pulsation excitation takes place in the tongue region of the volute and is thus placed on the downstream side of the model as indicated in Fig.2. The source can be expressed as the superposition of a onedimensional monopole and dipole [5, 6]. A monopole is implemented in terms of a mass source in the mass conservation equation. A dipole is in turn implemented by means of a momentum source in the momentum conservation equation. This leads to the following extended conditional equations for pressure and velocity at the source location:

$$p_i^{(n+1)} = \frac{1}{2}\left(\rho_i^n a_i^n \left(c_A - c_B\right) + \left(p_A + p_B\right)\right) + \left(p_s^{(n+1)} - p_s^{(n)}\right) \cdot \frac{a}{\omega \Delta x} \tag{9}$$

$$c_i^{(n+1)} = \frac{1}{2}\left(\frac{1}{\rho_i^n a_i^n}\left(p_A - p_B\right) + \left(c_A + c_B\right)\right) + \left(c_s^{(n+1)} - c_s^{(n)}\right) \cdot \frac{a}{\omega \Delta x} \tag{10}$$

with the transient source terms for a single frequency (usually f_{BP}) given by

$$p_s(t) = \hat{p}_s \cdot \left(cos\left(\omega t + \varphi_{p_s}\right)\right) \text{ and } c_s(t) = \hat{c}_s \cdot \left(cos\left(\omega t + \varphi_{c_s}\right)\right) \ . \tag{11}$$

In order to simulate the steady state in the modelled system in terms of mean flow, the characteristic head-curve of a pump is also implemented in the model as a "steady source". Therefore, the head-curve $H(Q)$ is first transformed into it's nondimensional analogue expressed by the pressure coefficient Ψ and volume flow coefficient Φ, which is then approximated by a polynomial $\Psi_{poly}(\Phi)$. At the location of this steady source the pressure coefficient corresponding to the current volume flow is then continuously evaluated and the respective specific fluid work $w_f = Hg$ is calculated. For the calculation of flow states located before (index 1) and after (index 2) the steady source the characteristic-based system of equations is extended by a mass balance and total pressure balance, which includes the work w_f induced by the steady source:

$$\rho_1 \cdot c_1 = \rho_2 \cdot c_2 \tag{12}$$

$$\frac{p_1}{\rho} + \frac{c_1^2}{2} + w_f = \frac{p_2}{\rho} + \frac{c_2^2}{2} \tag{13}$$

The steady source has successfully been validated, which is not shown here due to limited space.

2.2 Piping system

For the piping system an impedance model is applied, which represents the effective reflection coefficients on upstream and downstream side r_{pu}/r_{pd} by means of a cross sectional jump and a subsequent nonreflective boundary condition (nrBC), cf. Fig.2. The amplitudes of the measured reflection coefficients determine the area ratios which can be expressed by

$$\frac{A_{r,u}}{A_u} = \frac{d_{r,u}^2}{d_u^2} = \frac{1 - |r_{pu}|}{1 + |r_{pu}|} \quad \text{and} \quad \frac{A_{r,d}}{A_d} = \frac{d_{r,d}^2}{d_d^2} = \frac{1 - |r_{pd}|}{1 + |r_{pd}|} \ . \tag{14}$$

The phases of the reflection coefficients φ_r are adjusted by the length of the pipes l_d and l_u, to which they are related by the wavenumber $k = \frac{\omega}{a}$:

$$l_u = \frac{\varphi_{r_{pu}}}{2k} \quad \text{and} \quad l_d = \frac{\varphi_{r_{pd}}}{2k} \tag{15}$$

With such a domain termination those parts of a piping which are considered relevant can be simulated and the rest can be modelled as long as the effective reflection coefficient or termination impedance, which can be determined by means of measurements as described in Section 3, is known. Thus modelling as well as simulation effort is reduced. During the scope of this work only the piping sections directly connected to the pump (suction and discharge pipe) are simulated for validation purposes of the pump model.

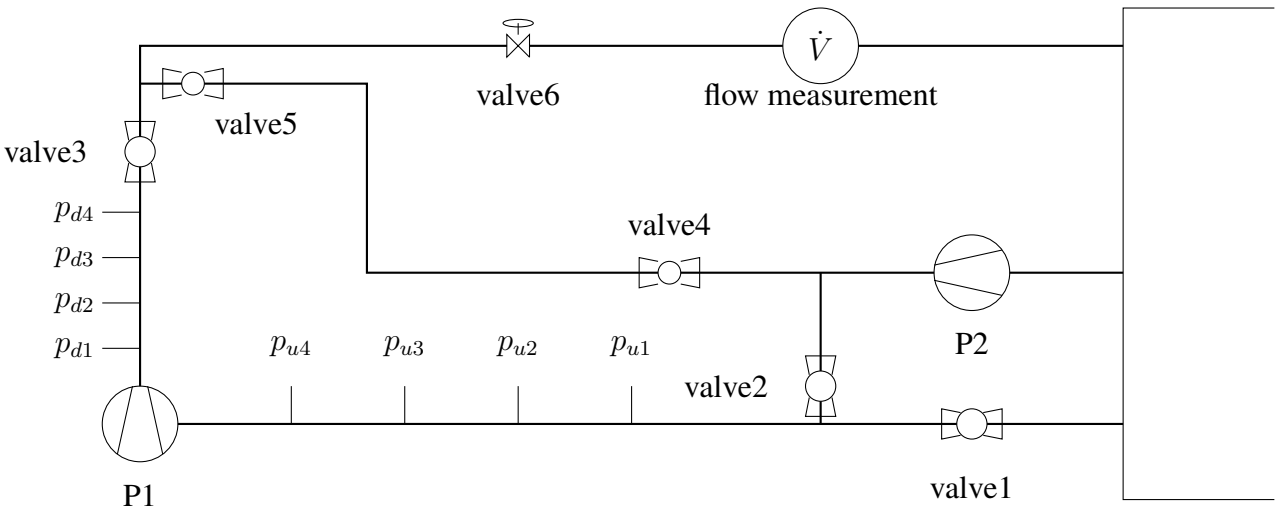

Figure 3: Experimental setup for the determination of acoustic pump parameters.

3. Determination of parameters

The acoustic parameters of the pump model are obtained by means of experiments. The experimental setup is shown in Fig.3. The pump under investigation is pump $P1$. On each side of $P1$ four piezoelectric pressure transducers are flush mounted for the measurement of upstream and downstream pulsations. The transient pressure signals are used to determine the Riemann invariants on the upstream and downstream side. The measured pressure amplitude at each sensor position can be expressed by $\underline{\hat{f}}$ and $\underline{\hat{g}}$:

$$\underline{\hat{p}}_i = \underline{\hat{f}} \cdot e^{-ikx_i} + \underline{\hat{g}} \cdot e^{ikx_i} \tag{16}$$

Applying Eq.(16) to each sensor position ($i = 1...4$) and solving the resulting overdetermined system of equations in the least square sense leads to the Riemann invariants. This applies to the upstream and downstream side. For a detailed description of the method refer to [16].

For the determination of the four-pole parameters of pump $P1$, measurements are carried out with $P1$ at standstill. Therefore, a second pump $P2$ is installed in the setup, which serves as an acoustic source. To determine the properties of an acoustic four pole at least two linearly independent acoustic states, which means two linearly independent sets of Riemann invariants have to be realised. A possibility to improve the validity of the results is the over-determination of four-pole data. Thereby, more than two linearly independent states are realised. During the scope of this work three different states (supercripts $i/ii/iii$) are realized by variation of valves 2, 3, 4 and 5. Thus the scattering matrix of pump $P1$ is determined by [11]:

$$\begin{pmatrix} \underline{t}_{ud} & \underline{r}_d \\ \underline{r}_u & \underline{t}_{du} \end{pmatrix} = \begin{pmatrix} \underline{\hat{f}}_u^i & \underline{\hat{f}}_u^{ii} & \underline{\hat{f}}_u^{iii} \\ \underline{\hat{g}}_d^i & \underline{\hat{g}}_d^{ii} & \underline{\hat{g}}_d^{iii} \end{pmatrix} \begin{pmatrix} \underline{\hat{f}}_d^i & \underline{\hat{f}}_d^{ii} & \underline{\hat{f}}_d^{iii} \\ \underline{\hat{g}}_u^i & \underline{\hat{g}}_u^{ii} & \underline{\hat{g}}_u^{iii} \end{pmatrix}^{-1} \tag{17}$$

In this work solely the blade passing frequency f_{BP} at nominal rotational speed of $n_{nom} = 2900\frac{U}{min}$ is considered. With a number of blades of $z = 6$ the blade passing frequency amounts to $f_{BP} = z \cdot n \cdot \frac{1}{60s} = 290Hz$. The four pole parameters at $f = 290Hz$ of the pump at standstill are shown in Fig.4. The geometrical parameters of the simple expansion chamber model are chosen to be $l_{ec} = 1.85\ m$ and $d_{ec} = 0.212\ m$ respectively. In combination with the pump's upstream diameter of $d_u = 0.0825\ m$ and downstream diameter of $d_d = 0.0703\ m$ the model four pole parameters result which are also shown in Fig.4. The maximum relative deviation in amplitude between pump and model parameters amounts to $\epsilon = 5\%$. The maximum difference in phase is $\Delta\varphi = 12°$. Thus,

the passive acoustic properties of the complex geometry of a centrifugal pump can be approximated satisfyingly by a simple expansion chamber model simulated in the time domain.
Once the scattering matrix is known, the source vector can easily be obtained by further measurements when pump $P1$ is running. For the first validation carried out in this work the pump is operated at an exemplary operating point with $\Phi = 0.027$ and $\Psi = 1.099$, which corresponds to the nominal operating point. Valves 4 and 5 are closed in this case. In order to preclude any influence of cavitation and thus ensure comparability of the transmission properties to the pump at standstill, the pump was operated at a high $NPSH_a$ value of $NPSH_a = 45\ m$. The $NPSH_a$ value is defined as

$$NPSH_a = \frac{p_{t,s} - p_v}{\rho \cdot g} \tag{18}$$

and quantifies the distance between the total pressure at the pump's suction piece $p_{t,s}$ and the vapour pressure p_v and thus the risk of cavitation. It is shown in the author's previous work that at $NPSH_a = 45\ m$ for the pump under investigation no influence of cavitation on occuring pressure pulsations is present [17]. It may thus be assumed that this $NPSH_a$ value is higher than the cavitation inception value $NPSH_i$, which is necessary to avoid any cavitation bubbles in the pump. The measured pressure amplitudes on the downstream side for this system configuration are shown in Fig.5.

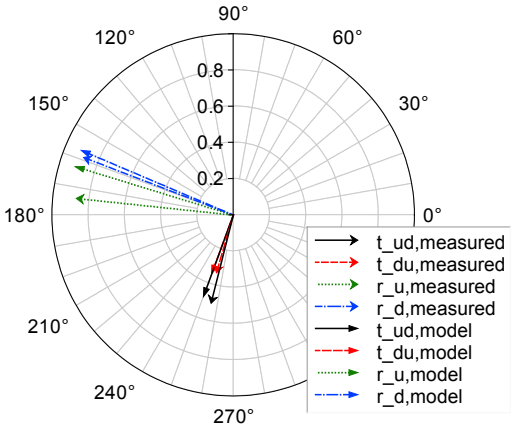

Figure 4: Measured scattering matrix parameters of the pump at $f = 290\ Hz$ and corresponding parameters of the expansion chamber model.

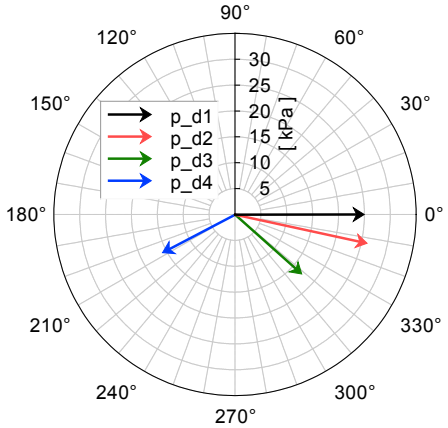

Figure 5: Measured downstream pressure amplitudes at $f = 290\ Hz$ for $P1$ at $\Phi = 0.027$ $\Psi = 1.099$.

The source vector can be determined by means of the Riemann invariants obtained for the operating pump using the transmission matrix $\bar{\bar{T}}$ and Eq.(5) or using the scattering matrix and the following relationship:

$$\begin{pmatrix} \hat{\underline{f}}_d \\ \hat{\underline{g}}_u \end{pmatrix} = \begin{pmatrix} \underline{t}_{ud} & \underline{r}_d \\ \underline{r}_u & \underline{t}_{du} \end{pmatrix} \begin{pmatrix} \hat{\underline{f}}_u \\ \hat{\underline{g}}_d \end{pmatrix} + \begin{pmatrix} \hat{\underline{f}}_s - \underline{r}_d\ \hat{\underline{g}}_s \\ -\underline{t}_{du}\ \hat{\underline{g}}_s \end{pmatrix} \tag{19}$$

For the pump $P1$ at the exemplary operating point using the four pole parameters obtained experimentally and illustrated in Fig.4 a complex source vector of

$$\begin{pmatrix} \hat{\underline{f}}_s \\ \hat{\underline{g}}_s \end{pmatrix} = \begin{pmatrix} 4326\ Pa \\ 9084\ Pa \cdot e^{i\ 75°} \end{pmatrix}\ , \tag{20}$$

is obtained. In terms of monopole (p) and dipole (c) source strength this amounts to (cf. Eq.(6–7))

$$\begin{pmatrix} \hat{\underline{p}}_s \\ \hat{\underline{c}}_s \end{pmatrix} = \begin{pmatrix} 11007\ Pa \\ 6693 \cdot 10^{-6}\ \frac{m}{s} \cdot e^{i\ -130°} \end{pmatrix}\ . \tag{21}$$

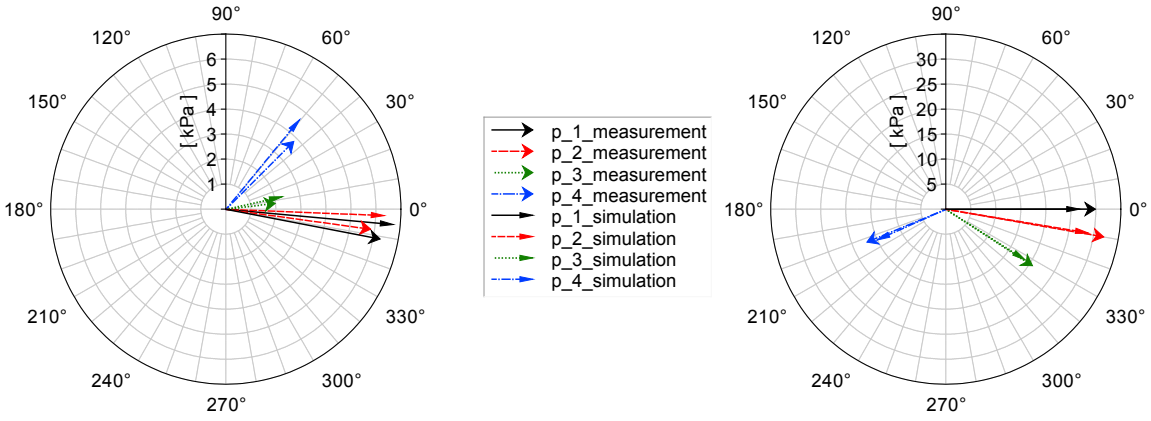

(a) (b)

Figure 6: Measured and simulated pressure amplitudes for $f = 290\ Hz$ at the four measurement positions on the upstream (a) and downstream side (b) of the pump

4. Numerical results

The parameters obtained in Section 3 are applied to the model described in Section 2. For a first validation of the model pump $P1$ was operated in the same operating point as before but the downstream impedance was changed by opening valve 5 (valve 4 is still closed), which results in overall higher amplitudes as well as slightly different phasing between the measurement points (cf. Fig.5 and Fig.6b). The simulated pressure amplitudes at the positions of the pressure transducers are evaluated and compared to the measured ones in Fig.6. On the downstream side (Fig.6b) no significant difference between measured and simulated phase can be observed. The relative deviation in amplitudes varies between $9\ \%$ and $12\ \%$. These are probably mainly due to differences in the modelled and the real source. The least root mean square error in the wave decomposition was always small ($\leq 5\%$) but present. The source vector is determined based on the Riemann invariants. Thus, errors in these affect the accuracy of the source vector. On the upstream side (Fig.6a) the phase error amounts to approximately $5°$ at each measurement point. The error in amplitude is also higher then on the downstream side and varies between $8\ \%$ and $20\ \%$. The higher errors on the upstream side are due to the transmission properties of the model which act between the source and the upstream side. The measured transmission properties could not exactly be reproduced by the simple expansion chamber model (cf. Section 3) which leads to higher deviations on the upstream side of the pump. The results show however that with a simple model in the time domain the acoustic properties of a centrifugal pump can be approximated with satisfactory agreement.

5. Conclusions

A onedimensional time-domain model of a centrifugal pump was presented. The model comprises the passive and active acoustic properties of a pump as well as the steady properties in terms of the characteristic curve. The acoustic parameters are obtained experimentally. A first validation showed that the acoustic transmission properties of a centrifugal pump can be approximated well by a simple expansion chamber model. In further investigations the determination of the geometrical parameter of the expansion chamber could be refined in order to further approach the real transmission properties of a pump. Furthermore nonlinear behaviour of cavitation bubbles could be investigated.

Acknowledgements

This work is based upon research carried out during the project "Flex-Power-Plant-Pumps" (funding code: 03ET7052C) funded by the Federal Ministry for Economic Affairs and Energy (BMWi), Germany and KSB AG.

REFERENCES

1. Brennen, C. E., *Hydrodynamics of pumps*, Cambridge University Press, Cambridge (2011).
2. Gülich, J. F., *Kreiselpumpen*, Springer-Verlag, Berlin Heidelberg New York (2004).
3. Keller, J., Parrondo, J., Barrio, R., Fernández, J., Blanco, E., Effects of the pump-circuit acoustic coupling on the blade-passing frequency perturbations, *Applied Acoustics*, **76**, 150–156, (2014).
4. Spence, R., Amaral-Texeira, J., A CFD parametric study of geometrical variations on the pressure pulsations and performance characteristics of a centrifugal pump, *Computers and Fluids*, **38**, 1243–1257, (2009).
5. Parrondo, J., Pérez, J., Barrio, R., González, J., A simple acoustic model to characterize the internal low frequency sound field in centrifugal pumps, *Applied Acoustics*, **72**, 59-64, (2011).
6. Parrondo-Gayo, J., González-Pérez, J., Fernández-Francos, J., The Effect of the operating point on the pressure fluctuations at the blade passage frequency in the volute of a centrifugal pump, *Journal of Fluids Engineering*, **124**, 784–790, (2002).
7. Rzentkowski, G., Zbroja, S., Experimental characterization of centrifugal pumps as an acoustic source at the blade-passing frequency, *Journal of Fluids and Structures*, **14**, 529–558, (2000).
8. Morgenroth, M., Weaver, D. S., Sound generation by a centrifugal volute pump at blade pass frequency, *Journal of Turbomachinery*, **120**, 736–743, (1998).
9. Brennen, E. C., A review of the dynamics of cavitating pumps, *Journal of Fluids Engineering*, **135**, (2013).
10. Bardeleben, M.J.R., *Acoustic characterization of a centrifugal pump using a two-port model*, PhD Thesis, McMaster University, Hamilton, (2005).
11. Han, Y., Smith, B. A. W., Luloff, B. V., Use of redundant sensors to determine the acoustic transfer matrix of a pump, *Flow-Induced Vibration*, **465**, 169–178, (2003).
12. Lucius, A., Brenner, G., Unsteady CFD simulations of a pump in part load conditions using scale-adaptive simulation, *International Journal of Heat and Fluid Flow*, **31**, 1113–1118, (2010).
13. Ruchonnet, N., *Multiscale computational methodology applied to hydroacoustic resonance in cavitating pipe flow*, PhD Thesis, École Polytechnique Fédérale de Lausanne, Lausanne, (2010).
14. Linkamp, A., Deimel, C., Brümmer, A., Skoda, R., Non-reflecting coupling method for one-dimensional finite difference/finite volume schemes based on spectral error analysis. *Computers and Fluids*, **140**, 334–346, (2016).
15. Polifke, W., Six Lectures on Thermoacoustic Combustion Instability, *21st CISM-IUTAM Int'l Summer School on "Measurement, analysis and passive control of thermoacoustic oscillations"*, Udine, Italy, (2015).
16. Edge, K., Johnston, D., The 'secondary source' method for the measurement of pump pressure ripple characteristics, Part 1 : description of method, *Journal of Power and Energy*, **204**, 33–40, (1990)
17. Lehr, C., Linkamp, A., Brümmer, A., Pulsationen an kavitierenden Kreiselpumpen, *Proceedings 43. Jahrestagung für Akustik*, Kiel, Germany, 6–9 März, (2017).